Nuclear Instruments and Methods in Physics Research B 267 (2009) 2467–2470

Contents lists available at ScienceDirect

Nuclear Instruments and Methods in Physics Research B

journal homepage: www.elsevier.com/locate/nimb

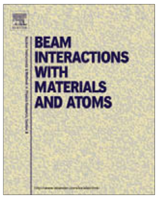

Study of the electronic structures of oxygen doped in $LiBaF_3$ crystal [☆]

Hailing Qiao [a], Tingyu Liu [a,b,*], Qiren Zhang [a], Fan Cheng [a], Xiuwen Zhou [a]

[a] College of Science, University of Shanghai for Science and Technology, 516 JunGong Road, Shanghai 200093, China
[b] Shanghai Key Laboratory of Contemporary Optics System, 200093, China

ARTICLE INFO

Article history:
Received 2 May 2009
Received in revised form 27 May 2009
Available online 6 June 2009

PACS:
61.72.Ji
61.72.Bb
71.15.−m
71.20.Ps

Keywords:
$LiBaF_3$ crystal
Oxygen doped
$[O_F' + V_F^{\cdot}]$
Electronic structures
Absorption band

ABSTRACT

The most likely substituting positions of impurity oxygen ions in $LiBaF_3$ crystals are studied using the general utility lattice program (GULP). The calculated results indicate that the main defect model is $[O_F' + V_F^{\cdot}]$ in the O:$LiBaF_3$ crystal. The electronic structures of the $LiBaF_3$ crystal with the defect $[O_F' + V_F^{\cdot}]$ are calculated using the DV-Xα method. It can be concluded from the electronic structures that the $LiBaF_3$ crystal with the defect $[O_F' + V_F^{\cdot}]$ will exhibit a 217–280 nm absorption band and the impurity oxygen will decrease core-valence luminescence yield.

1. Introduction

$LiBaF_3$ crystal is known as a scintillation material. It has been applied in vacuum ultraviolet optical lithography, X-ray storage phosphor and other luminescent devices [1–3]. This inorganic material is remarkable because of the presence of both core valence luminescence (CV) and self trapped-exciton luminescence (STE) under gamma irradiation whereas only the STE luminescence is present under neutron or alpha-irradiation, which makes it suitable for applications as a thermal neutron detector [4]. The CV luminescence is found between 190 and 220 nm. This is a basis to developing fast scintillators. However, the presence of oxygen impurities is a restricting factor for this usage [5], which changes the sensitivity of this material to ionizing radiation and optical properties.

The experiments on pure and oxygen doped $LiBaF_3$ crystal have been performed by Shiran et al. [6]. For oxygen doped crystal, there exhibits some new absorption bands in the region of 208–280 nm in the UV part of the spectrum. The presence of new absorption bands may be related to the impurity oxygen ions. In the process of crystal growth, it is found that oxygen ions are easily incorporated into the crystal and enhance the absorption band in 180–230 nm range [7]. The O:$LiBaF_3$ crystal has attracted extensive attention, because additional absorption bands are overlapped with the useful fast core-valence luminescence, resulting in a decrease in the light yield. In an earlier study on the structures of oxygen-doped BaFCl and BaF_2 by photoluminescence-detected electron paramagnetic resonance [8,9], it is claimed that the oxygen may substitute for fluorine and combine with a next nearest fluorine vacancy forming the defect cluster $[O_F' + V_F^{\cdot}]$ in the crystal. However, there is little direct experimental and theoretical evidence on the existent form of oxygen ions in the $LiBaF_3$ crystal. The main compensating mechanism of oxygen ions in $LiBaF_3$ crystals and the corresponding electronic structures have not been studied in detail up to now.

Computer simulation provides a useful means of studying how the properties of $LiBaF_3$ are affected by doping ions. In a previous paper, computer simulation is successfully used to study of the influence of oxygen incorporation on crystal growth in $LiBaF_3$ crystal [10]. In order to clarify the charge compensating mechanism in oxygen-doped $LiBaF_3$ crystals, the possible defect models in O:$LiBaF_3$ crystals are studied using the general utility lattice

---

[☆] Project supported by the Foundation of Shanghai Municipal Education Committee, China (Grant No. 09YZ210) and the Shanghai Leading Academic Discipline Project (S30502)

[*] Corresponding author. Address: College of Science, University of Shanghai for Science and Technology, 516 JunGong Road, Shanghai 200093, China. Tel.: +86 021 55272483.
E-mail address: liutyyxj@163.com (T. Liu).

0168-583X/$ - see front matter © 2009 Elsevier B.V. All rights reserved.
doi:10.1016/j.nimb.2009.05.072

Table 1
Empirically derived potential parameters used in $LiBaF_3$ crystal.

Short-range potential parameters					Shell parameters			
Interactions	A(ev)	$\rho(10^{-10}m)$	$C(Å^6eV)$	References	Ions	Y(e)	$K(Å^{-2}eV)$	References
$Li^+–F^-$	113.720	0.3654	0.000	[10]	Li^+	1.0		[10]
$Ba^{2+}–F^-$	2190.01	0.3068	0.000	[10]	Ba^{2+}	2.0		[10]
$F^-–F^-$	1127.70	0.2753	15.83	[10]	F^-	−1.378	24.36	[10]
$O^{2-}–F^-$	464.540	0.3362	22.10	[10]	O^2	−2.040	6.3	[10]

program (GULP). The electronic structures of oxygen-doped in $LiBaF_3$ crystal with the optimal defect models are calculated using DV-Xα software and the effects of doped oxygen on the optical properties of the crystal are discussed in this paper.

2. The cluster models and calculation methods

2.1. The possible defect cluster models

There are various possibly charge compensating mechanisms existing in O:$LiBaF_3$ crystals, which correspond to different defect clusters and substitution reactions. Impurity oxygen ions can enter the $LiBaF_3$ crystal in two forms: occupying fluorine lattice sites and interstitial positions.

If the impurity oxygen ion occupies the fluorine lattice site, it will induce an excess negative charge in $LiBaF_3$ crystal. There are three charge compensatory forms $V_F^{\cdot}$, $Li_i^{\cdot\cdot}$ and $Ba_{Li}^{\cdot}$, which will form the complex defect clusters $[O_F' + V_F^{\cdot}]$, $[O_F' - Li_i^{\cdot\cdot}]$ and $[O_F' - Ba_{Li}^{\cdot}]$, respectively. The three compensating mechanisms can be demonstrated by defect chemical Eqs. (1)–(3), respectively.

$$LiO_2 + LiBaF_3 \rightarrow O_F' + V_F^{\cdot} + BaF_2 + LiF \tag{1}$$

$$LiO_2 + LiBaF_3 \rightarrow O_F' + Li_i^{\cdot\cdot} + BaF_2 + LiF \tag{2}$$

$$LiO_2 + LiBaF_3 \rightarrow O_F' + Ba_{Li}^{\cdot} + LiF \tag{3}$$

By analyzing the formation energy and binding energy of the defect clusters, the optimal compensating mechanism could be found.

2.2. The calculation methods

The lattice simulations are performed using the GULP program [11] that is based upon the Mott–Littleton methodology for accurate modeling of defective lattices. The program GULP optimizes the structure with respect to the asymmetric unit fractional coordinates and cell strains, using analytical symmetry-adapted first and second derivatives within a Newton–Raphson procedure starting from the exact Hessian matrix [12–14]. An important feature of these calculations is the modeling of defects. The simplification of the Mott-Littleton method is to divide the crystal lattice that surrounds the defect into three regions known as I, 2a, and 2b. In order to confirm the optimal position of the impurity oxygen in the crystal, possible positions that impurity oxygen ions may occupy are simulated. The potential parameters used in the calculations are listed in Table 1.

Table 2
Initial basis sets and the funnel potential parameters (FPWPs).

Ion	Frozen core	Orbits for basis functions	FPWP(arb. units)		
			V_0	R_1	R_2
Li^+		1s,2s,2p	−3.0	1.5	2.0
Ba^{2+}	1s–5s	5p,5d,6s	−3.0	2.5	3.0
F^-	1s	2s,2p,3s	−2.9	2.1	2.5
O^{2-}	1s	2s,2p,3s	−8.0	1.6	3.0

After the optimal defect clusters in the crystal are determined by the GULP program, the molecular-cluster model with the framework of the fully relativistic self-consistent Direc-Slater theory, using a numerically discrete variational (DV-Xα) method [15], was adopted to study the electronic structures for the perfect crystal and the $LiBaF_3$ crystal with the optimal defect clusters.

In embedding cluster scheme method, one suitable ionic cluster is chosen. The eigenfunction can be obtained by solving the Kohn-Sham equations:

$$h_{ks}\varphi_i(r) = \left[-\frac{\nabla^2}{2} - \sum_q \frac{Z_q}{|r - R_q|} + \int \frac{\rho(r)}{|r - r'|} dr' + V_{xc} \right] \times \varphi_i(r) = \varepsilon_i \varphi_i(r), \tag{4}$$

where the first part is the kinetic energy, the second part is the attractive Coulomb potential between nuclei in all molecules and electrons and the third part is the Coulomb potential of electrons. V_{xc} is the exchange-correlation potential [16].

The original basis sets are composed of free ionic and atomic orbits, and these basis sets are optimized in an iterative process according to the occupation of molecular orbitals, until the difference between two terms in the Hamiltonian is a minimum. The initial basis sets and the funnel potential well chose for the calculations are listed in Table 2. V_0 denotes the depth of the atom potential well, R_1 and R_2 show the minimum radius of atoms and the cutoff radius. The advantages of this method are that it has a high calculation precision with a relatively less workload and suits calculation for large molecules and solid systems.

3. Calculated results and discussion

3.1. Optimal position of impurity oxygen in $LiBaF_3$ crystal

In order to confirm the optimal positions of impurity oxygen ions in $LiBaF_3$ crystal, possible positions where the impurity oxy-

Table 3
Energies of isolated point defects and defect clusters.

Isolated point defect		Defect clusters		
Defect	Formation energy(eV)	Configuration	Formation energy (eV)	Binding energy (eV)
O_F'	−22.094	$[O_F' + V_F^{\cdot}]$	−22.181	4.323
$V_F^{\cdot}$	4.136	$[O_F' + Ba_{Li}^{\cdot}]$	−28.326	0.804
$Ba_{Li}^{\cdot}$	−5.428	$[O_F' + Li_i^{\cdot}]$	−25.228	0.309
$Li_i^{\cdot}$ (1/2,0,0)	−3.443			
Li_i (1/2,1/4,1/4)	−3.798			
$Li_i^{\cdot}$ (1/4,1/4,1/4)	−3.928			